Matrine improves skeletal muscle atrophy by inhibiting E3 ubiquitin ligases and activating the Akt/mTOR/FoxO3α signaling pathway in C2C12 myotubes and mice

LI CHEN[1,2], LINLIN CHEN[1,2], LILI WAN[1], YAN HUO[1], JINLU HUANG[1], JIE LI[1], JIN LU[1], BO XIN[1,3], QUANJUN YANG[1] and CHENG GUO[1,2]

[1]Department of Pharmacy, Shanghai Jiao Tong University Affiliated Sixth People's Hospital, Shanghai 200233; [2]School of Medicine, Shanghai Jiaotong University, Shanghai 200240; [3]Shanghai University of Traditional Chinese Medicine, Shanghai 200135, P.R. China

Received November 26, 2018; Accepted May 14, 2019

DOI: 10.3892/or.2019.7205

Abstract. Skeletal muscle wasting is a feature of cancer cachexia that increases patient morbidity and mortality. Matrine, the main bioactive component of *Sophora flavescens*, has been approved for the prevention and therapy of cancer cachexia in China. However, to the best of our knowledge, its mechanism in improving muscle wasting remains unknown. The present study demonstrated that matrine increases muscle fiber size and muscle mass in an *in vivo* CT26 colon adenocarcinoma cachexia mouse model. Concurrently, other cachexia symptoms, including body and organ weight loss, were alleviated. In *in vitro* experiments, matrine substantially improved C2C12 myoblast differentiation with or without dexamethasone treatment. In addition, matrine reduced C2C12 myotube atrophy and apoptosis induced by dexamethasone, tumor necrosis factor α and conditioned medium. Two E3 ubiquitin ligases, muscle RING-finger containing protein-1 and muscle atrophy Fbox protein, which are specifically expressed in wasting skeletal muscle, were also significantly downregulated ($P<0.05$) by matrine both in C2C12 myotubes and skeletal muscle. Furthermore, matrine increased the phosphorylation of Akt, mTOR and FoxO3α in the atrophying C2C12 myotube induced by dexamethasone. In conclusion, matrine can alleviate muscle atrophy and improve myoblast differentiation possibly by inhibiting E3 ubiquitin ligases and activating the Akt/mTOR/FoxO3α signaling pathway.

Correspondence to: Professor Cheng Guo or Dr Quanjun Yang, Department of Pharmacy, Shanghai Jiao Tong University Affiliated Sixth People's Hospital, 600 Yishan Road, Shanghai 200233, P.R. China
E-mail: guopharm@126.com
E-mail: myotime@126.com

Abbreviations: MuRF1, muscle RING-finger containing protein-1; MAFbx, muscle atrophy Fbox protein; CFDA, China Food and Drug Administration; Dex, dexamethasone; TNFα, tumor necrosis factor α; CSA, cross-sectional area; CM, conditioned medium

Key words: cancer cachexia, skeletal muscle, matrine; E3 ubiquitin ligase, Akt/mTOR/FoxO3α

Introduction

Cancer cachexia is a multifactorial syndrome characterized by weight loss, muscle atrophy and anorexia, with or without adipose tissue loss (1,2). In total, 50-80% of patients with advanced cancer develop cachexia and it is widely accepted to be indirectly responsible for ≥20% of all cancer-associated mortalities (3). Furthermore, cancer cachexia can cause resistance to comprehensive treatment, increase the incidence of adverse reactions, reduce patient quality of life, and increase morbidity and mortality (4,5). The pathogenesis mechanism of cancer cachexia is complicated and there are no effective means for preventing skeletal muscle wasting. A number of studies have focused on early diagnosis (6,7) and the development of new drugs to delay cachexia progression (8,9).

Muscle atrophy is the most specific characteristic of cancer cachexia and is induced by an imbalance between muscle protein synthesis and degradation (10). Skeletal muscle protein degradation is primarily regulated by the ubiquitin-proteasome pathway under wasting conditions (11,12). Two E3 ubiquitin ligases, muscle RING-finger containing protein-1 (MuRF1) and muscle atrophy Fbox protein (MAFbx), are specifically expressed in atrophying skeletal muscle and mediate the degradation of muscle protein (13,14). The expression of these E3 ubiquitin ligases is mediated by several signaling pathways, including PI3K/Akt, NF-κB/IκB kinase and myostatin/activin receptor type-2B signalling (15-18). During muscle atrophy, PI3K/Akt pathway activity decreases, leading to activation of the FoxO3α transcription factor and expression of E3 ubiquitin ligases (19). In addition, muscle protein synthesis is mediated by several myogenic genes, including the myogenic differentiation antigen (MyoD) family of transcription factors, including MyoD, myogenin (MyoG), myogenic factor 5 (Myf5) and myogenic regulatory factor 4 (Mrf4) (20). Reagents that can block protein degradation and/or activate protein synthesis are expected to be beneficial therapies for skeletal muscle atrophy.

Matrine is approved by the China Food and Drug Administration (CFDA) for the prevention and treatment of cancer cachexia. As the main active component of *Sophora flavescens*, matrine has been widely used in Traditional Chinese Medicine for thousands of years. In recent decades, matrine has been verified to exhibit broad efficacy against hepatitis (21), cardiac injury (22), fibrotic diseases (23) and cancer (24-27), which occurs via regulation of Akt/FoxO3α, NF-κB, JAK-STAT and mTOR pathways. Previously, it has been reported that matrine improves cancer cachexia symptoms and partly preserves skeletal muscle mass in mice. This effect was mostly attributed to matrine's anti-inflammatory activity (28). However, evidence demonstrates that inflammation is not the main driving force of cancer cachexia-induced muscle wasting (29,30). Therefore, an in-depth study of matrine's intrinsic mechanism for preserving muscle mass is required.

The aim of the present study was to evaluate the effect of matrine on skeletal muscle atrophy and clarify the underlying mechanism. It was first evaluated whether matrine-treatment could ameliorate skeletal muscle atrophy in an *in vivo* cancer cachexia mouse model induced by CT26 colon adenocarcinoma. Subsequently, it was elucidated whether matrine-treatment could improve C2C12 myoblast differentiation and alleviate myotube atrophy induced by dexamethasone (Dex), tumor necrosis factor α (TNFα) or conditioned medium (CM). In addition, the effect of matrine on E3 ubiquitin ligases and their associated signaling pathways was analyzed.

Materials and methods

Cell culture and differentiation. The CT26 colon adenocarcinoma and C2C12 cell lines were obtained from the American Type Culture Collection (Manassas, VA, USA). These cells were confirmed to be without mycoplasma contamination by using a color one-step mycoplasma detection kit [Yeasen Biotechnology (Shanghai) Co., Ltd., Shanghai, China]. The cells were maintained in Dulbecco's modified Eagle's medium (DMEM; Corning Life Sciences, Corning, NY, USA) supplemented with 10% heat-inactivated fetal bovine serum (Zhejiang Tianhang Biotechnology Co., Ltd., Hangzhou, China), 100 U/ml penicillin and 100 μg/ml streptomycin. The cells were cultured in an incubator at 37˚C in a humidified atmosphere of 5% CO_2. Myotubes were induced by culturing the C2C12 cells in DMEM with 2% horse serum (Gibco; Thermo Fisher Scientific, Inc., Waltham, MA, USA) for 3-5 days, replacing the medium every 24 h.

Establishment of C2C12 myotube atrophy models and treatments. Three C2C12 myotube atrophy models were established, according to previous studies (31-33). Briefly, C2C12 myoblasts were differentiated to myotubes by culturing in 2% horse serum at 37˚C. Dex (National Institute for the Control of Pharmaceutical and Biological Products, Beijing, China) or TNFα (Novus Biologicals, LLC, Littleton, CO, USA) were then added to the media for 48 h at 100 μM and 50 ng/ml, respectively. For the third model, the myotubes were incubated for 48 h in CM consisting of 33% 'cachexia liquid' and 66% fresh DMEM with 2% horse serum; this CM was replaced every 24 h. The 'cachexia liquid' was acquired as follows; when CT26 cells reached 90% confluence, their culture medium was replaced with 2% horse serum (differentiation medium) and the supernatant was collected as 'cachexia liquid' after 48 h. For the investigation of myoblast differentiation and myotube atrophy, matrine (Shanghai EFE Biological Technology Co., Ltd., Shanghai, China) was added to the culture medium at 0.1 and 0.2 mM for 48 h at 37˚C. For the signalling pathway investigation, 0.1 mM matrine was added for 48 h at 37˚C and 10 nM wortmannin (MedChemExpress, Monmouth Junction, NJ, USA) was added to culture medium for 48 h at 37˚C.

Cell Counting Kit-8 (CCK-8) assay. The CCK-8 (Dojindo Molecular Technologies, Inc., Kumamoto, Japan) assay was performed according to the manufacturer's protocol. Briefly, CT26 or C2C12 cells were seeded in 96-well plates at 3,000-5,000 cells/well. Matrine (97%) was added at different concentrations (0.1, 0.3, 0.89, 2.68, 8.05 and 24.16 mM for CT26 cells, and 0.001, 0.004, 0.012, 0.037, 0.111, 0.333 and 1 mM for C2C12) for 48 h. Subsequently, 10 μg/ml CCK-8 regent was added and incubated at 37˚C for 1 h. The absorbance was measured at 490 nm with a Synergy™ HT Multi-Mode Microplate Reader (BioTek Instruments, Inc., Winooski, VT, USA).

Immunofluorescence and determination of C2C12 myotube diameter and myotube fusion index. After being treated with or without matrine (100 μM) and Dex (100 μM) for 48 h at 37˚C, the myotubes were washed with cold PBS three times and were fixed with 4% paraformaldehyde at room temperature. The cells were permeabilized by treatment with 0.5% Triton X-100 for 20 min. The myotubes were washed with PBS and blocked in 5% bovine serum albumin (Beijing Solarbio Science and Technology Co., Ltd., Beijing, China) for 1 h at room temperature (25±2˚C). The myotubes were incubated with primary antibodies against myosin heavy chain (MHC; cat. no. sc-376157; 1:200), MyoD (cat. no. sc-71629; 1:150), MuRF1 (cat. no. sc-398608; 1:150) and MAFbx (cat. no. sc-166806; 1:150) overnight at 4˚C, which were all purchased from Santa Cruz Biotechnology, Inc. (Dallas, TX, USA). The myotubes were then incubated with Alexa Fluor 488-conjugated (cat. no. 4408S; 1:1,000) and Alexa Fluor 594-conjugated secondary antibodies (cat. no. 8889S; 1:1,000) at 4˚C overnight, which were both from Cell Signalling Technology, Inc. (Danvers, MA, USA). DAPI (5 μg/ml; Beijing Solarbio Science and Technology Co., Ltd.) was used to stain the nuclei for 5 min at room temperature. Images of the C2C12 myotubes were obtained under a fluorescence microscope equipped with a digital camera (Olympus Corporation, Tokyo, Japan; magnification, x100 and x200). A minimum of six representative images were selected and 150 sets of myotube data were measured per group by CellSens standard software (version 1.16; Olympus Corporation).

Animal cancer cachexia model and matrine treatment. All procedures involving animals and their care in this study were approved by the Animal Care Committee of Shanghai Sixth People's Hospital (Shanghai, China) in accordance with institutional requirements and Chinese government guidelines for animal experiments. Six-week-old male mice

(weight, 20±1.5 g) were housed in a controlled environment (25±2˚C; 12 h light/12 h dark cycle; relative humidity of ~50-60%) and provided standard laboratory chow and water *ad libitum*. The mouse cancer cachexia model bearing CT26 tumor was established as previously described (34,35). Briefly, 40 mice were divided randomly into four groups with ten mice per group. The normal control (NC) group included mice without CT26 inoculation that received normal saline treatment. The normal mice treated with matrine (NC + Mat) group consisted of mice without CT26 inoculation that received matrine-treatment. The cancer cachexia (CC) group included mice with CT26 inoculation that received normal saline treatment. The cancer cachexia mice treated with matrine (CC + Mat) group consisted mice with CT26 inoculation that received matrine-treatment. The CT26 tumor suspension (~2×10^6 cells) was injected subcutaneously into the right flanks of the mice. Ten days after CT26 inoculation, 50 mg/kg matrine was given via intraperitoneal injection. The food intake, body weights, and longest and shortest tumor diameters were recorded every 2 days. The tumor weights were calculated using the following formula: Weight (mg)=0.52 x (L x S^2), where L is the longest diameter and S is the shortest diameter. The longest diameter of the CT26 tumors did not exceed 1.5 cm during the experiment. A total of 21 days after tumor inoculation, the mice were euthanized. The heart, liver, spleen, lungs, kidneys, epididymal fat, gastrocnemius muscle and tibialis anterior muscle were dissected, weighed and snap frozen in liquid nitrogen.

Table I. Primer sequences used for reverse transcription-polymerase chain reaction.

Gene name	Direction	Sequence (5'-3')
MuRF1	Forward	TGCCTACTTGCTCCTTGTGC
	Reverse	CACCAGCATGGAGATGCAGT
MAFbx	Forward	ACGTCGCAGCCAAGAAGAG
	Reverse	ATGGCGCTCCTTCGTACTTC
MHC I	Forward	GCTGAGGCCCAGAAACAAG
	Reverse	TTCCACGATGGCGATGTTC
MHC IIa	Forward	ACTTTGGCACTACGGGGAAAC
	Reverse	CAGCAGCATTTCGATCAGCTC
MHC IIb	Forward	CTTTGCTTACGTCAGTCAAGGT
	Reverse	AGCGCCTGTGAGCTTGTAAA
MHC IIx	Forward	GCGAATCGAGGCTCAGAACAA
	Reverse	GTAGTTCCGCCTTCGGTCTTG
Myostain	Forward	CCAGGACCAGGAGAAGATGG
	Reverse	GGATTCCGTGGAGTGCTCAT
GAPDH	Forward	TGGTCGTATTGGGCGCCTGGT
	Reverse	TCGCTCCTGGAAGATGGTGA

MuRF1, muscle RING-finger containing protein-1; MAFbx, muscle atrophy Fbox protein; MHC, myosin heavy chain.

Hematoxylin-eosin staining and determination of the myofiber cross-sectional area (CSA). A total of three fresh gastrocnemius muscles were dissected randomly from each group, fixed with GD fixative (v/v=1:19) (Servicebio, Wuhan, China; cat. no. G1111) for 12 h at room temperature, embedded with paraffin, sectioned into 4 μm-thick slices and stained with hematoxylin for 8 min (Servicebio; cat. no. G1004) and eosin-phloxine (Servicebio; cat. no. G1001) for 1 min at room temperature. The muscle sections were observed under a light microscope (Olympus Corporation; magnification, x200). Myofiber CSAs were calculated using CellSens software (version 1.16; Olympus Corporation), and a minimum of six images and 180 sets of data were acquired per group.

RNA isolation and reverse transcription-quantitative polymerase chain reaction (RT-qPCR). Total RNA from mice gastrocnemius, tibialis anterior and C2C12 myotubes were extracted using RNAiso reagent (Takara Bio Inc., Otsu, Japan). cDNA was synthesized using HiScript II Q RT SuperMix for qPCR (cat. no. R223-01; Vazyme Biotech Co. Ltd., Nanjing, Jiangsu, China) with the following procedure: 37˚C for 15 min and 85˚C for 5 sec. qPCR was performed with ChamQ™ Universal SYBR qRT-PCR Master mix (cat. no. Q711-02; Vazyme Biotech Co. Ltd.). qPCR and data analysis were conducted on a StepOnePlus™ Real-Time PCR system (Thermo Fisher Scientific, Inc.), according to the manufacturer's protocol. The qPCR amplifications consisted of 40 cycles of 95˚C for 30 sec, 95˚C for 15 sec and 62˚C for 30 sec. The $2^{-\Delta\Delta Cq}$ method (36) was used for quantification. All data were from three independent experiments. GAPDH was used as the internal control gene. The primers were designed, synthesized and ultra-purified by Sangon Biotech Co. Ltd., Shanghai, China (Table I).

Western blotting. Myotubes and gastrocnemius muscle tissue were lysed using RIPA buffer (Thermo Fisher Scientific, Inc.). Total protein was quantified with a BCA kit (Beyotime Institute of Biotechnology, Haimen China). Subsequently, 50 μg denatured protein per lane was subjected to SDS-PAGE on 10% polyacrylamide gels and then transferred to polyvinylidene difluoride membranes. Following blocking with 5% skim milk in TBS containing 0.05% Tween-20 for 1 h at room temperature, the membranes were incubated with primary antibodies against MuRF1 (cat. no. sc-398608; 1:500), MAFbx (cat. no. sc-166806; 1:500), phosphorylated (p)-Akt (cat. no. sc-81433; 1:500), Akt (cat. no. sc-81434; 1:500), p-FoxO3α (cat. no. sc-101683; 1:500), FoxO3α (cat. no. sc-48348; 1:500), p-mTOR (cat. no. sc-293133; 1:250), mTOR (cat. no. sc-517464; 1:250; all from Santa Cruz Biotechnology, Inc.) and GAPDH (cat. no. 5174S; 1:1,000; Cell Signaling Technology, Inc.) at 4˚C overnight. After washing with PBS, the corresponding fluorescently labelled secondary antibodies (catalog nos. 926-68020 and 926-68021, 1:3,000; LI-COR Biosciences, Lincoln, NE, USA) were incubated with the membranes at room temperature for 1.5 h. The membranes were imaged on an Odyssey® CLx Infrared Imaging system (LI-COR Biosciences). Image Studio 5.0 software (LI-COR Biosciences) was used for measuring integrated optical densities.

Statistical analysis. Statistical analyses were performed using SPSS version 19.0 (IBM Corp., Armonk, NY, USA).

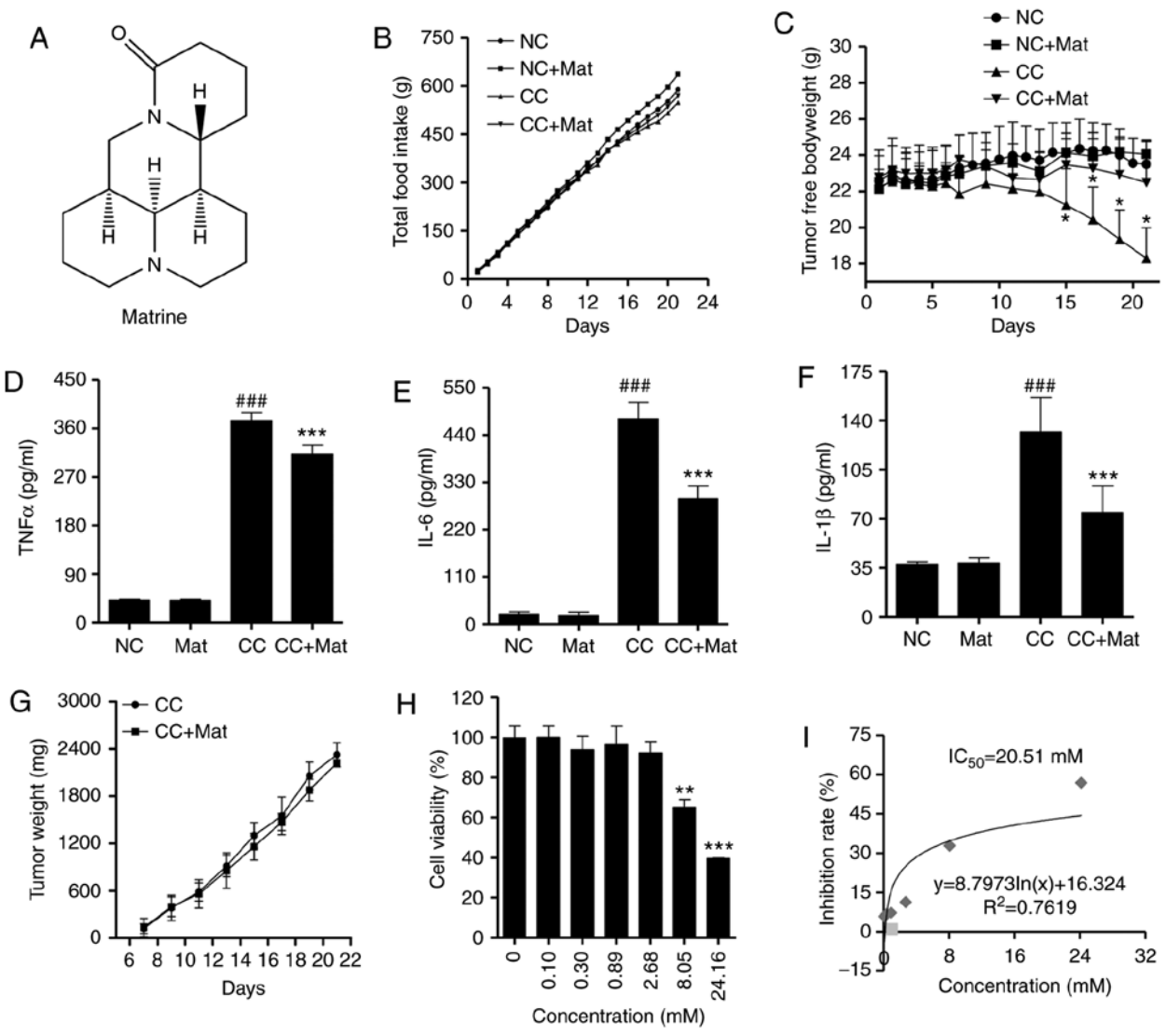

Figure 1. Effect of matrine on CT26-induced cancer cachexia symptoms, and CT26 tumor growth and cell proliferation. (A) Chemical structure of matrine. (B) Cumulative food intake of mice with different treatments in each group (n=10). (C) Mice tumor free bodyweight during the experiment (n=10). Levels of (D) TNFα, (E) IL-6 and (F) IL-1β in mice serum (n=10). (G) Calculated weight of CT26 tumors (n=10). (H) Effect of matrine on the cell viability of CT26 cells (n=4). (I) Inhibition curve of matrine to CT26 cell proliferation. Data are presented as the mean ± standard deviation. Statistical significance was determined by one-way ANOVA. ###P<0.001 vs. NC. *P<0.05, **P<0.01, ***P<0.001 vs. CC. NC, negative control; Mat, matrine; CC, cancer cachexia.

Significance was determined using one-way ANOVA. For comparisons among multiple groups, post-hoc pairwise comparisons were performed using Tukey's multiple-comparison tests. All values are expressed as the mean ± standard deviation (n≥3). P<0.05 was considered to indicate a statistically significant difference.

Results

Matrine improves cancer cachexia symptoms in CT26-bearing mice and exhibits limited effects on CT26 cell proliferation. To evaluate the anti-cachexia effect of matrine (Fig. 1A), a classic CT26 colon adenocarcinoma-bearing murine model was established. The tumors were palpable by the seventh day post-inoculation. Mice bearing CT26 tumors presented with early cancer cachexia symptoms, including decreased food intake from day 12 (Fig. 1B). Total body weights were not significantly different until day 18 in the CT26-bearing mice compared with the negative control (data not shown). However, the free-tumor body weights (total body weight minus tumor weight) were significantly different from day 15 (P<0.05; Fig. 1C). Based on a previous study (28), the mice were intraperitoneally injected with matrine at 50 mg/kg. Matrine-treatment demonstrated a positive effect on the body weights but no influence on food intake.

The organ and tissue weights also suggested less wasting in the cancer cachexia matrine-treatment group compared with in the cancer cachexia group (Table II). The mass loss in the gastrocnemius and tibialis anterior muscles was also reversed with matrine-treatment. In addition, matrine significantly decreased the serum concentrations of inflammatory cytokines, including TNFα (Fig. 1D), IL-6 (Fig. 1E), and IL-1β (Fig. 1F), which are known cachectins (10).

CT26 tumor growth was not significantly inhibited following matrine-treatment in mice (Fig. 1G). To determine the anticancer activity of matrine in CT26 cells, a CCK-8 assay

Table II. Organ and tissue weights of mice in different treatment groups.

Organ or tissue	NC	NC + Mat	CC	CC + Mat
Heart, mg	112.67±7.93	107.75±6.33	70.66±5.45[a]	97.15±7.55[c]
Liver, mg	1,144.65±120.15	1,025.17±362.05	1,403.86±131.29[a]	1,379.98±153.37
Spleen, mg	101.68±10.34	91.16±8.46	328.76±43.98[a]	263.30±47.78[c]
Lung, mg	137.54±9.89	136.17±13.71	128.66±11.89	126.41±9.93
Kidney, mg	355.46±25.84	361.17±23.66	315.55±33.13[a]	354.42±25.32[c]
Epididymal fat, mg	576.74±58.72	611.58±71.64	131.59±48.42[b]	271.56±84.27[d]
Gastrocnemius, mg	298.42±25.10	310.56±19.86	202.52±28.50[b]	263.05±29.34[e]
Tibialis anterior, mg	99.77±11.03	116.41±19.06	66.05±15.58[b]	94.49±12.93[d]

Data are presented as the mean ± standard deviation (n=10). Statistical significance was determined by one-way ANOVA. [a]P<0.05, [b]P<0.001 vs. NC group. [c]P<0.05, [d]P<0.01, [e]P<0.001 vs. CC group. NC, normal control. CC, cancer cachexia. Mat, matrine.

was performed to determine the viability of CT26 cells with or without matrine-treatment. The data demonstrated that when the cells were treated with ≥8.05 mM matrine for 48 h, the cell viability significantly decreased in a concentration-dependent manner (Fig. 1H). The calculated IC_{50} of matrine was 20.51 mM in CT26 cells (Fig. 1I). All of these results indicate a limited anticancer effect of matrine. Thus, the anti-cachexia effect of matrine appears to occur predominantly through the alleviation of body weight and muscle wasting, rather than anticancer effects.

Matrine improves skeletal muscle atrophy in cachexia by inhibiting E3 ubiquitin ligase expression. To determine whether the beneficial effect of matrine on muscle wasting resulted from alleviation of skeletal muscle atrophy, histological analysis of gastrocnemius muscle was performed. Compared with that of the NC group, the CC group exhibited myofiber atrophy, presenting as random loose fiber arrangements and large inter-fiber gaps (Fig. 2A). The gastrocnemius myofibers of the cachexia mice also demonstrated a sharp decrease in CSA, with most myofibers having a value of 200-300 μm^2. Following matrine-treatment, the shape and arrangement of the myofibers normalized, and there was a marked CSA increase, with most myofibers exhibiting a value of 400-500 μm^2 (Fig. 2B). Compared with that in the CC group, there was a 70% increase in CSA in the CC + Mat group (Fig. 2C), which supported the muscle weight increases. No negative influence of matrine on the gastrocnemius muscle of normal mice was observed.

Subsequently, the mRNA levels of two E3 ubiquitin ligases, MAFbx and MuRF1, in both gastrocnemius and tibia anterior muscle were quantified by RT-qPCR. The mRNA expression levels of both genes were significantly elevated more than ten-fold in the cachexia mice compared with the NC group. Notably, matrine-treatment significantly downregulated the mRNA levels of both E3 ubiquitin ligases (Fig. 2D). Consistent with the mRNA expression data, western blots demonstrated that the protein expression levels of MuRF1 and MAFbx in gastrocnemius muscle were significantly inhibited by matrine-treatment compared with the CC group (Fig. 2E). Although there were differences between mice, matrine significantly decreased the levels of the two E3 ubiquitin ligases in the cachexia skeletal muscle.

Matrine demonstrates no toxicity to C2C12 myocytes and myotubes <0.2 mM. In order to determine the concentrations of matrine that are non-toxic to C2C12 myocytes and myotubes, a CCK-8 assay was performed. The data demonstrated that the IC_{10} of matrine toward C2C12 myocytes is 0.203 mM (Fig. 3A and B), indicating no significant toxicity at <0.203 mM. In addition, RT-qPCR analysis indicated that 0.2 mM matrine exhibited no significant overall influence on the mRNA expression of MHC, a major structural protein of myotubes. However, matrine treatment at 0.1 mM significantly upregulated the expression of MHC Ib (Fig. 3C). For MHC IIa (Fig. 3D) and IIb (Fig. 3E), there were no significant changes with matrine-treatment at any concentration. In addition, matrine (0.4 mM) significantly inhibited the expression of MHC Ib and MHC IIx (Fig. 3C and F).

Matrine promotes C2C12 myoblast differentiation with/without Dex. Double immunofluorescence staining of MHC and MyoD was used to investigate the effect of matrine on normally differentiated or Dex-stimulated C2C12 myoblasts. As presented in Fig. 4A, the myotubes, but not the undifferentiated myoblasts, were stained for MHC and MyoD. Furthermore, matrine increased myotube diameters at 0.1-0.4 mM (Fig. 4B). Notably, the myoblasts fused into giant and atypical myotubes when matrine was used at 0.4 and 0.8 mM, with higher matrine concentrations demonstrating increased fusion (Fig. 4C). However, compared with that in the other matrine-treatment groups, MyoD expression was lower in the 0.8 mM matrine-treatment group.

It was identified that Dex can significantly inhibit differentiation of C2C12 myoblasts, since there was less myotube formation in the Dex-treated groups. Furthermore, the formed myotubes in the Dex-treated groups were shorter and exhibited fewer nuclei (Fig. 5A). With matrine-treatment at 0.1-0.4 mM, the myotube diameters and fusion indexes increased (Fig. 5B and C). These results indicate that matrine can increase the differentiation of C2C12 myoblasts, even in the presence of Dex, which impairs their differentiation. However,

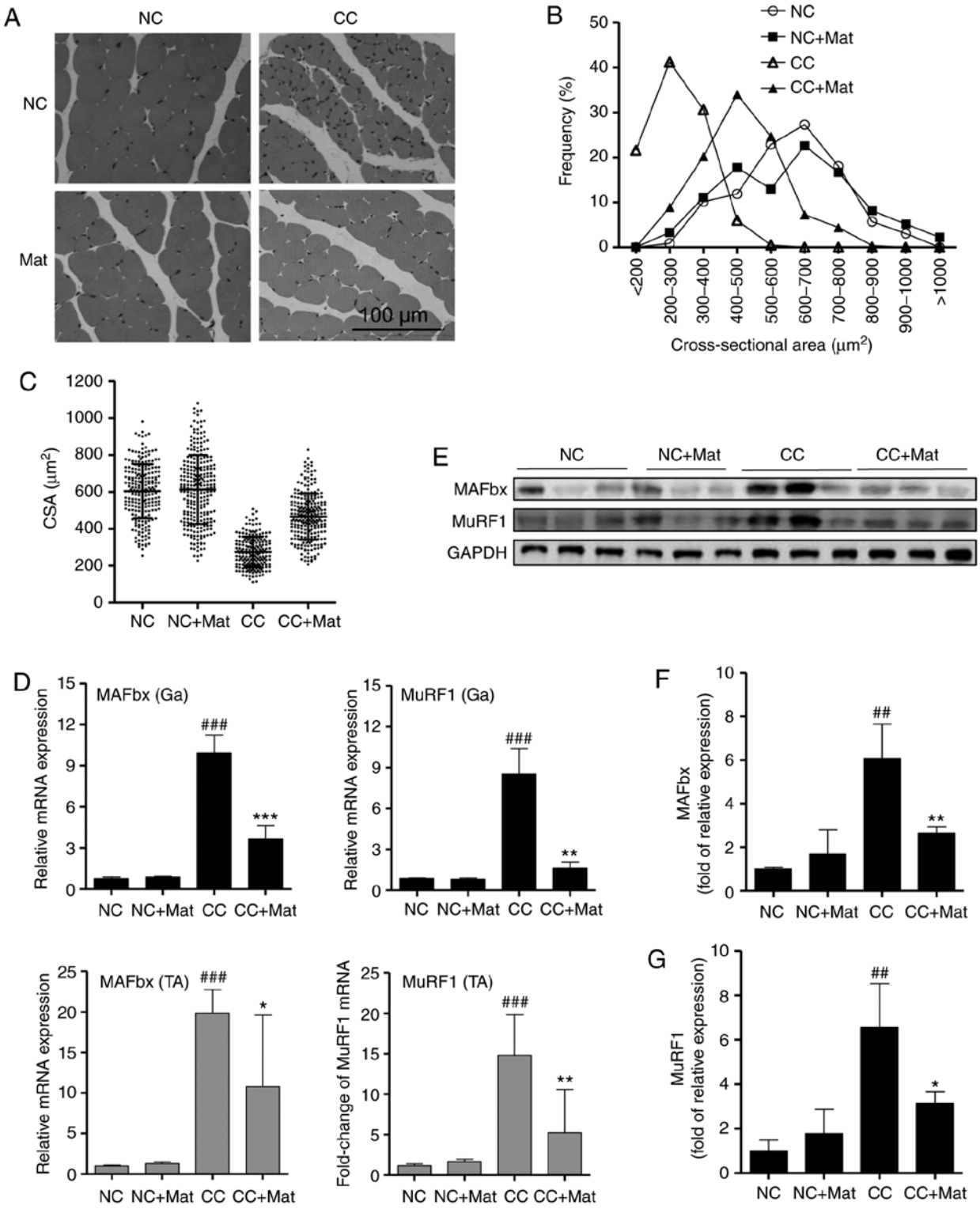

Figure 2. Matrine alleviates mice myofibers atrophy by down-regulating the expression of E3 ubiquitin ligase. (A) Hematoxylin-eosin staining of myofibers in mice gastrocnemius. (B) The statistical results of myofiber CSA distribution in each group (n>180 per group). (C) Mean muscle fibers CSA. (D) Reverse transcription-quantitative polymerase chain reaction detected MAFbx and MuRF1 mRNA expression in mice Ga (upper panels) and TA (lower panels) (n=6). (E) Representative western blot images of MuRF1 and MAFbx in mice Ga. (F and G) Statistical results of the western blot analysis (n=3). Data are presented as the mean ± standard deviation. Statistical significance was determined by one-way ANOVA. $^{\#\#}$P<0.01, $^{\#\#\#}$P<0.001, vs. NC. *P<0.05, **P<0.01, ***P<0.001 vs. CC. NC, negative control; Mat, matrine; CC, cancer cachexia; CSA, cross-sectional area; Ga, gastrocnemius; TA, tibialis anterior; MuRF1, muscle RING-finger containing protein-1; MAFbx, muscle atrophy Fbox protein.

there was no significant difference in fusion index between the Dex + Mat 0.8 mM and Dex groups. In addition, compared with that of the other matrine-treatment groups, the Dex + Mat 0.8 mM group demonstrated lower MyoD expression. This suggests matrine can increase myoblast differentiation when used up to 0.4 mM.

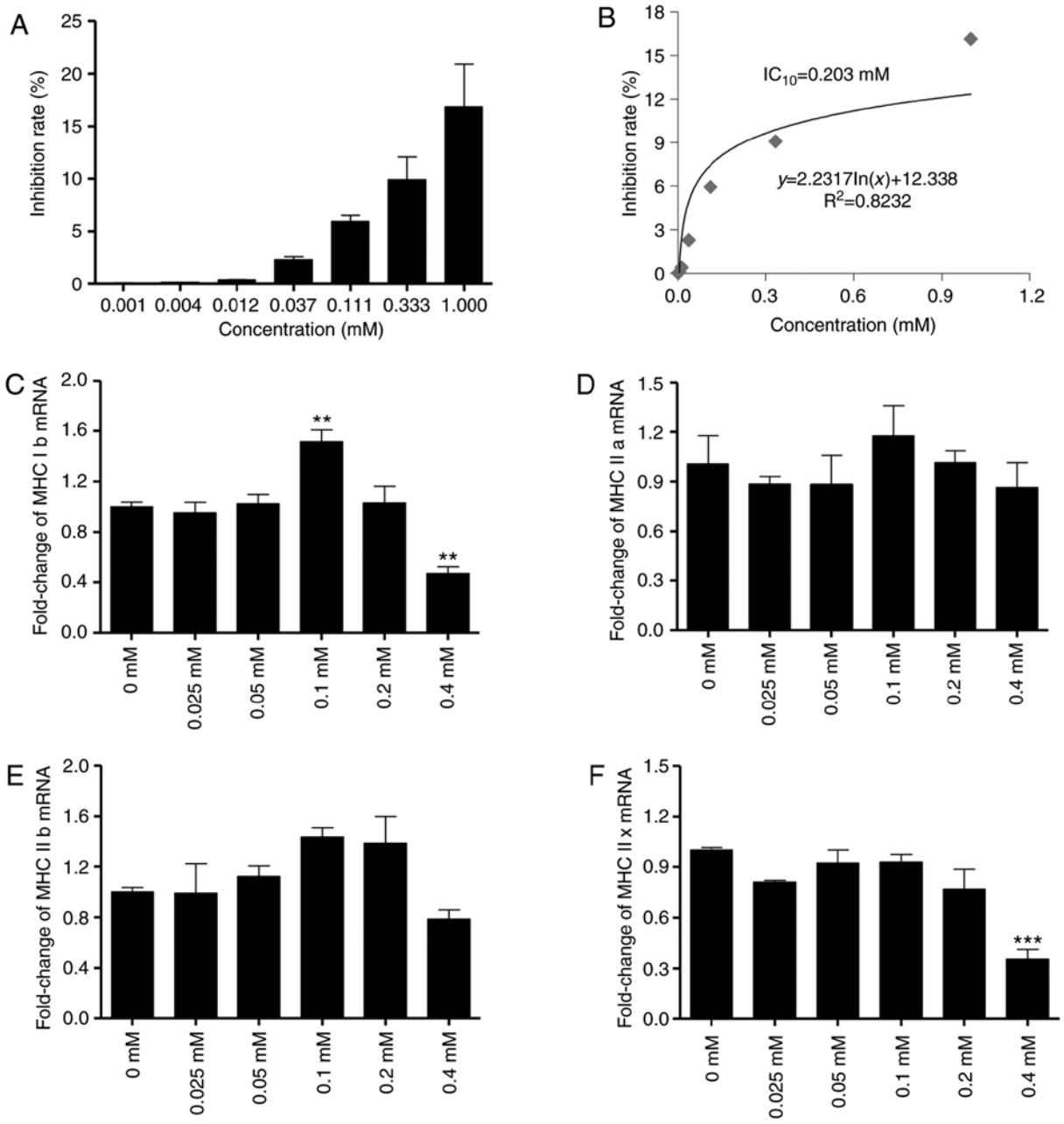

Figure 3. Matrine exhibits no significant cytotoxic effect to C2C12 myocytes and myotubes. (A) Inhibition rate and (B) IC_{10} of matrine to C2C12 myocytes for 48 h determined by CCK-8 assay (n=4). (C-F) The mRNA levels of MHC subfamily proteins, including (C) MHC Ib, (D) MHC IIa, (E) MHC IIb and (F) MHC IIx, in myotubes following treatment with matrine (0.025, 0.05, 0.1, 0.2 and 0.4 mM) were analyzed by reverse transcription-quantitative polymerase chain reaction (n=3). Data are presented as the mean ± standard deviation. Statistical significance was determined by one-way ANOVA. $^{**}P<0.01$, $^{***}P<0.001$ vs. untreated control. MHC, myosin heavy chain.

Matrine increases atrophic C2C12 myotube diameters and inhibits Dex-induced upregulation of E3 ubiquitin ligases. Despite having confirmed that matrine promotes C2C12 myoblast differentiation, whether it can stabilize myotubes in the presence of impairment factors remains unknown. After 3-5 days of differentiation and myotube formation, 100 μM Dex, 50 ng/ml TNFα or CM were added for 48 h to induce myotube apoptosis and atrophy. Dex-treatment resulted in the apoptosis and atrophy of formed myotubes, since discontinuous MHC staining was visible. TNFα- and CM- treatment also resulted in extensive myotube damage. Matrine demonstrated protective effects at both 0.1 mM (Mat-L) and 0.2 mM (Mat-H; Fig. 6A). The diameters of most normal myotubes ranged between 9-15 μm, while they ranged between 5-11 μm after being treated with Dex, TNFα or CM (Fig. 6B and C). With matrine co-treatment, the myotube diameters significantly improved, with values of 7-15 μm. There was no effect of matrine on the morphology of normal myotubes, indicating the absence of toxicity on formed myotubes.

Western blotting and immunofluorescence for MAFbx and MuRF1 (Fig. 7) also supported the ability of matrine to protect myotubes under Dex-induced myotube conditions. Dex-treatment significantly upregulated MAFbx and MuRF1 (Fig. 7A). Matrine (0.1 mM) decreased expression of MAFbx and MuRF1 by 27 and 43%, respectively. These results are consistent with the *in vivo* experimental findings

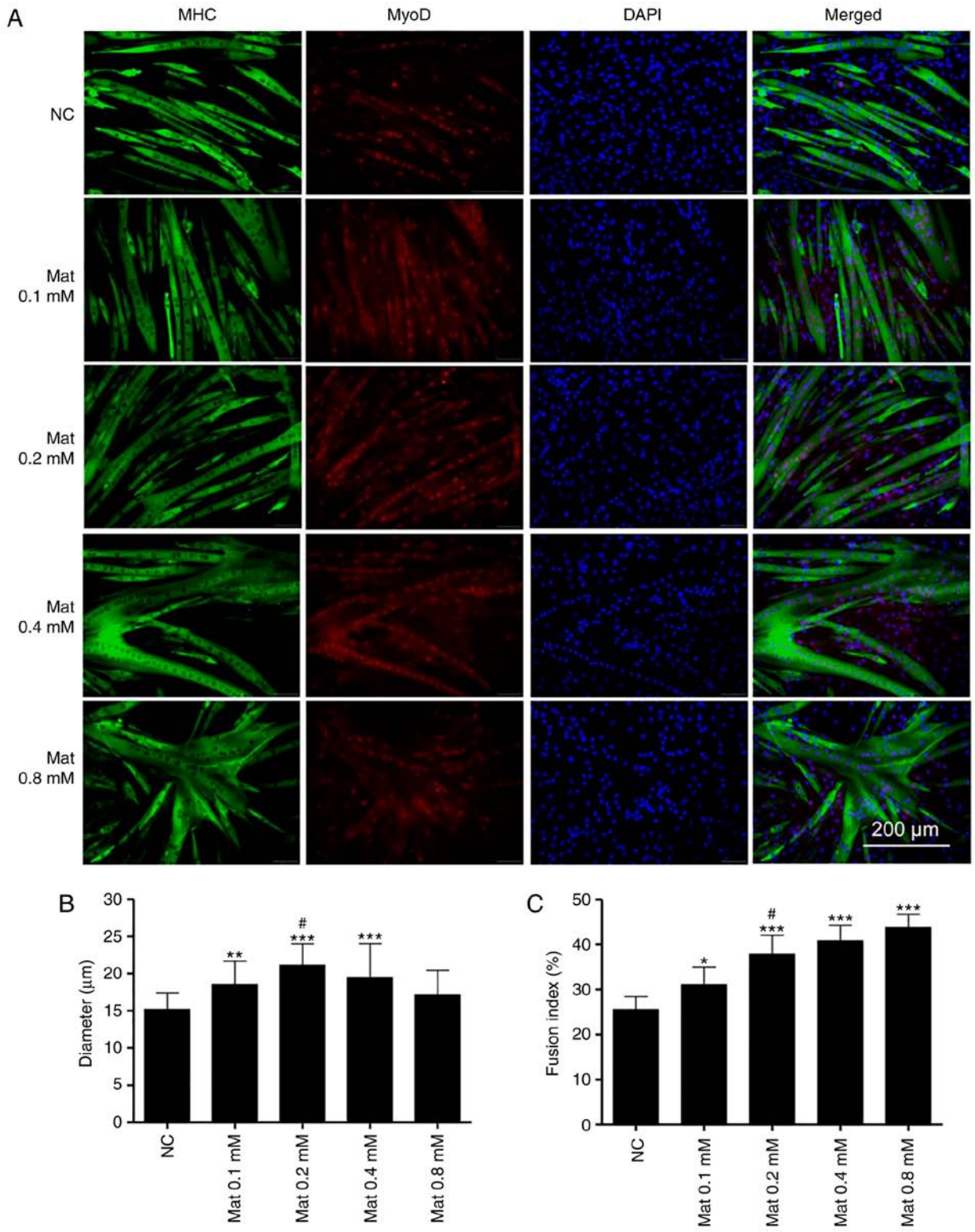

Figure 4. Matrine promotes C2C12 myoblasts differentiation and fusion. (A) Immunofluorescence staining of MHC (green), MyoD (red) and DAPI (blue) in C2C12 myotubes. After getting close to 80% confluence, C2C12 myoblasts were treated with or without the indicated concentrations of matrine in differential medium for 72 h. Quantification of C2C12 myotubes (B) mean diameter (3-5 measures per myotube; n>150 per group) and (C) fusion index. Myotubes fusion index was calculated by the proportion of nuclei in myotubes to the total nuclei (n=6). Data are presented as the mean ± standard deviation. Statistical significance was determined by one-way ANOVA. $^{\#}$P<0.05 vs. 0.1 mM Mat. *P<0.05, **P<0.01, ***P<0.001 vs. NC. MHC, major histocompatibility complex; NC, negative control; Mat, matrine; MyoD, myogenic differentiation antigen.

where matrine downregulated the expression of MAFbx and MuRF1 in cachexia mice skeletal muscle. In addition, matrine exhibited no significant influence on the expression of these two E3 ubiquitin ligases in normal myotubes. Furthermore, it was identified that matrine significantly decreased the mRNA level of myostatin (Fig. S1), an upstream regulator of E3 ubiquitin ligases, which was significantly upregulated by following treatment with Dex.

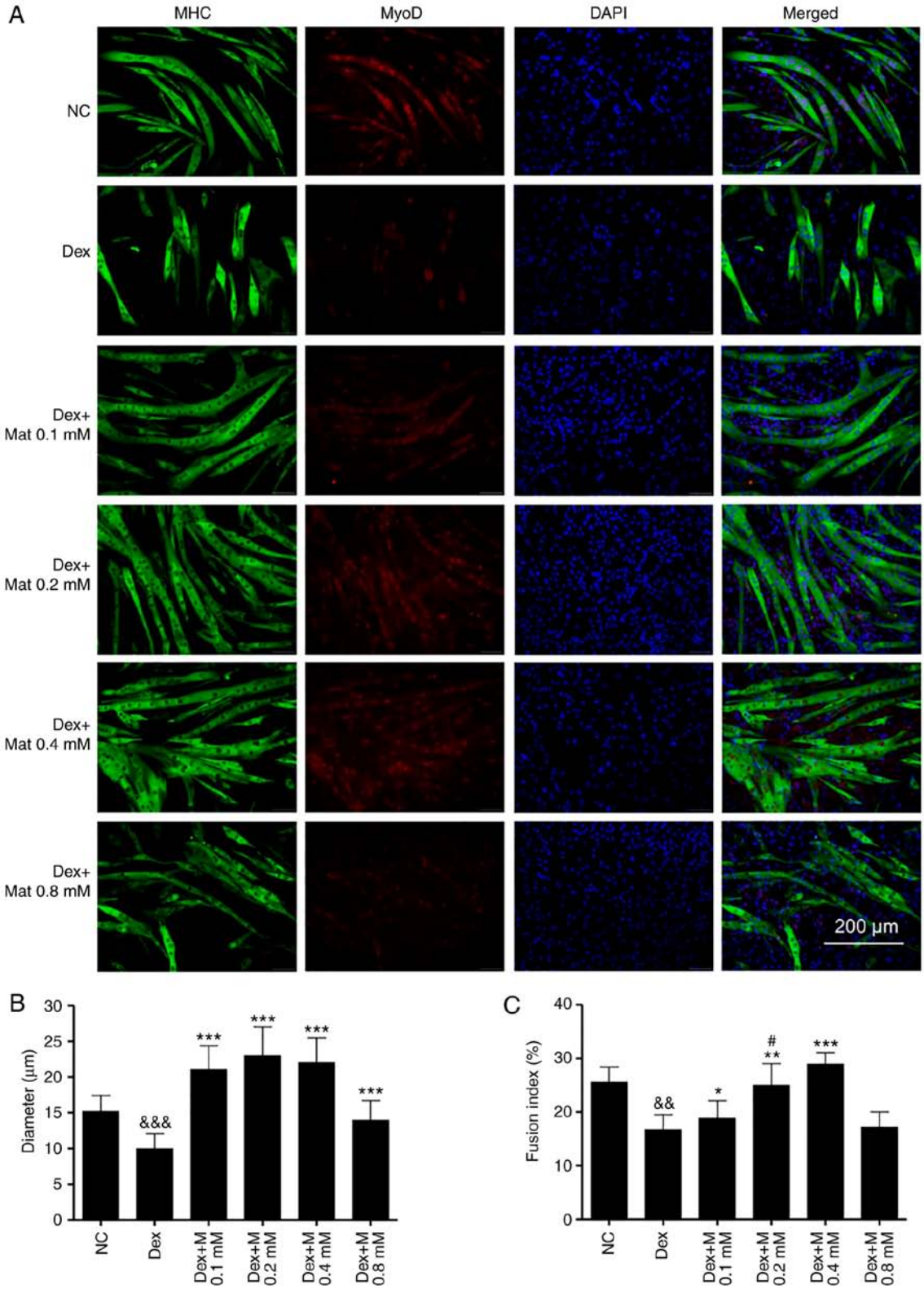

Figure 5. Matrine improves the inhibitory effect of dexamethasone on C2C12 myoblasts differentiation. (A) Immunofluorescence staining of MHC (green), MyoD (red) and DAPI (blue) in C2C12 myotubes. C2C12 myoblasts were treated with Dex combined with or without Mat in differential medium for 72 h. Quantification of C2C12. (B) Mean myotubes diameter (3-5 measures per myotube; n>150 per group) and (C) Fusion index (n=6). Data are presented as the mean ± standard deviation. Statistical significance was determined by one-way ANOVA. $^{\#}$P<0.05 vs. Dex + 0.1 mM Mat. *P<0.05, **P<0.01, ***P<0.001 vs. Dex. $^{\&\&}$P<0.01, $^{\&\&\&}$P<0.001 vs. NC. MHC, myosin heavy chain.

The western blotting data was then corroborated using immunofluorescence. The images revealed that MAFbx and MuRF1 could not be detected in normal C2C12 myotubes. However, particularly with the Dex-treatment group, both E3 ubiquitin ligases demonstrated higher fluorescence. Co-treatment with matrine substantially decreased the

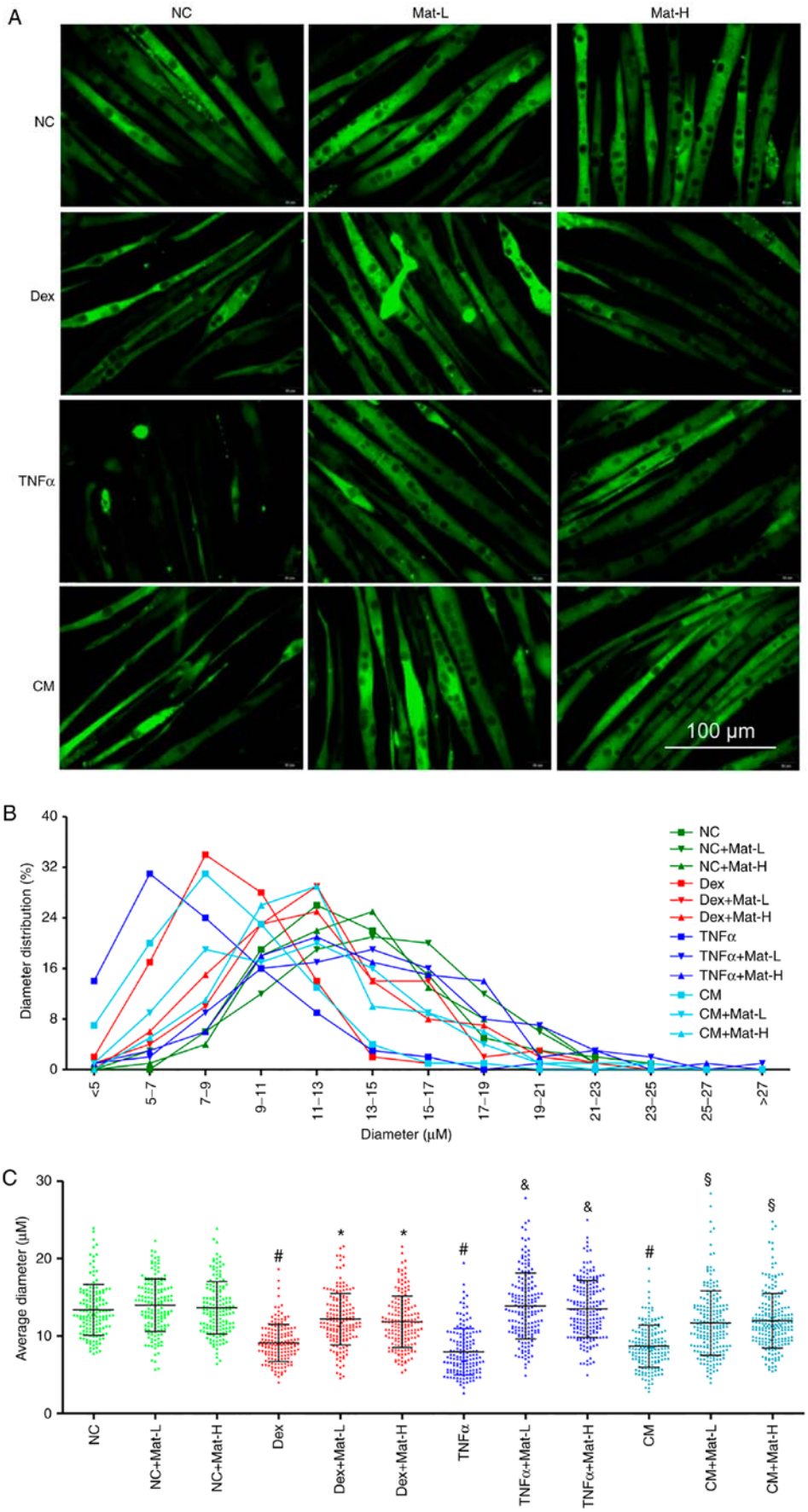

Figure 6. Anti-atrophic effect of matrine on C2C12 myotubes. (A) Immunofluorescence staining of MHC in C2C12 myotubes. C2C12 myotubes (B) diameter distribution and (C) mean diameter in each group. Ten images were selected from each group and each myotube was measured three to five times along the axis. In total, >50 myotubes were determined and ≥150 sets of data were collected. Data are presented as the mean ± standard deviation. Statistical significance was determined by one-way ANOVA. $^{\#}$P<0.001 vs. NC. *P<0.001 vs. Dex. $^{\&}$P<0.001 vs. TNFα. §P<0.001 vs. CM. NC, negative control; Dex, dexamethasone; Mat-L, 100 μM matrine; Mat-H, 200 μM matrine; CM, conditioned medium.

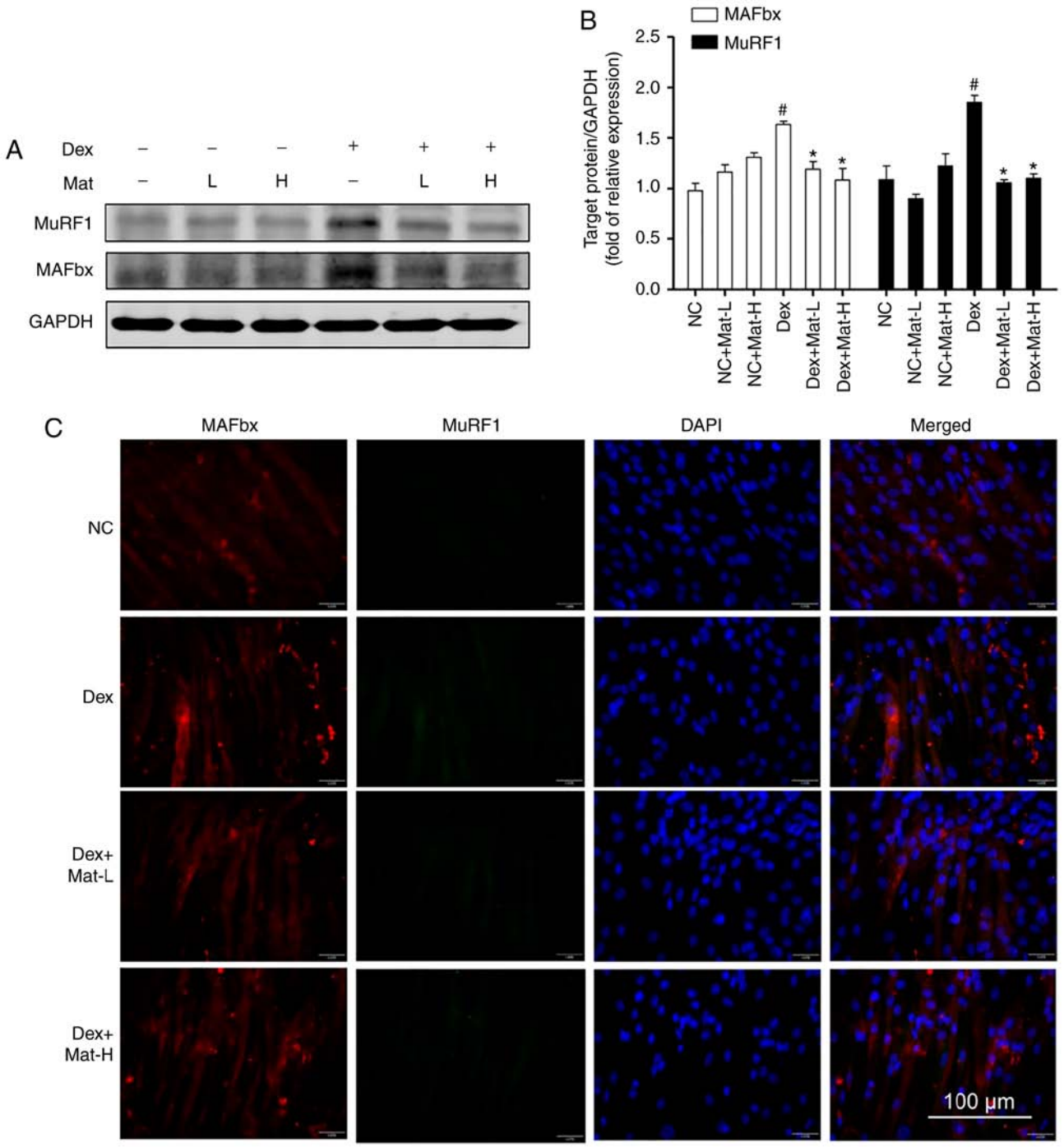

Figure 7. Matrine inhibits the expression of MAFbx and MuRF1 in C2C12 myotubes. (A) Representative western blot images of MuRF1 and MAFbx. (B) Quantitation of western blot analysis (n=3). (C) Immunofluorescence staining of MAFbx (red) and MuRF1 (green) in C2C12 myotubes (n=3). Data are presented as the mean ± standard deviation. Statistical significance was determined by one-way ANOVA. #P<0.001 vs. NC. *P<0.001 vs. Dex. NC, negative control; Dex, dexamethasone; Mat-L, 100 μM matrine; Mat-H, 200 μM matrine; MuRF1, muscle RING-finger containing protein-1; MAFbx, muscle atrophy Fbox protein.

expression of both E3 ubiquitin ligases, with little observable difference between the two concentrations of matrine.

Effect of matrine on the Akt/mTOR/FoxO3α signaling pathway in C2C12 myotubes. When myotubes were treated with 100 μM Dex for 48 h, accompanied by the upregulated expression of the two E3 ubiquitin ligases, a significant decrease was also identified in the relative phosphorylation of Akt, mTOR and FoxO3α. Treatment with matrine at 0.1 mM for 48 h reversed this effect on Akt, FoxO3α, and mTOR phosphorylation (P<0.05; Fig. 8). However, compared with the treatment with Dex and matrine, the additional treatment with 10 nM wortmannin (a PI3K inhibitor) for 48 h diminished the effect of matrine by decreasing the phosphorylation of Akt, mTOR and FoxO3α, accompanied by the upregulation of MAFbx and MuRF1. This indicates that the anti-atrophic effect of matrine was attenuated by inhibition of the Akt/mTOR/FoxO3α signaling pathway. Therefore, these results suggest that

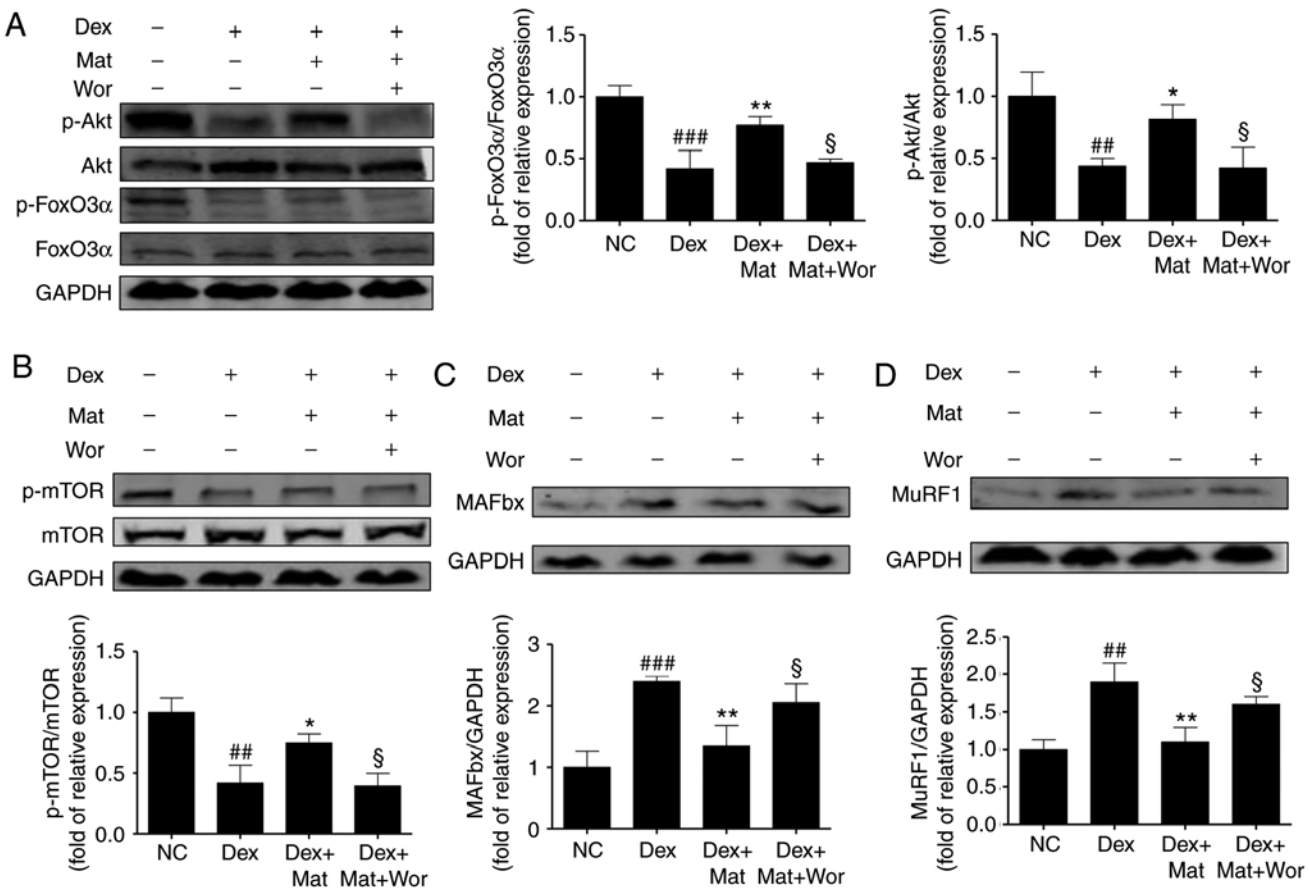

Figure 8. Effect of matrine on the Akt/mTOR/FoxO3α signalling pathway in C2C12 myotubes. Representative western blot images and densitometric quantification of the associated phosphorylated levels of (A) FoxO3α, Akt, (B) mTOR, (C) MAFbx and (D) MuRF1 in C2C12 myotubes. Dex, matrine and wortmannin were added to culture medium for 48 h at 100 μM, 0.1 mM and 10 nM, respectively. Data are presented as the mean ± standard deviation (n=3). Statistical significance was determined by one-way ANOVA. *P<0.05, **P<0.01 vs. Dex. $^{\#\#}$P<0.01, $^{\#\#\#}$P<0.001 vs. NC. §P<0.05 vs. Dex + Mat. NC, negative control; Dex, dexamethasone; Mat, matrine; Wor, wortmannin; p, phosphorylated; MuRF1, muscle RING-finger containing protein-1; MAFbx, muscle atrophy Fbox protein.

matrine-treatment upregulates anabolism and downregulates catabolism of muscle-specific proteins.

Discussion

Body composition analysis has demonstrated that patients with cancer cachexia lose 30% of their body weight and their muscle mass decreases by ~75% (37). Skeletal muscle atrophy has been associated with poor prognosis and suboptimal responses (5,38). However, until recently, there has been no effective medicine to treat cancer cachexia-induced muscle atrophy. Matrine is approved by the CFDA for the prevention and treatment of cancer cachexia; however, to the best of our knowledge, its mechanism of activity on skeletal muscle remains unknown. The present study investigated the anti-muscle atrophy effects and mechanisms of matrine activity both *in vitro* and *in vivo*. Matrine significantly improved the diameter and fusion index of C2C12 myotubes. Matrine also normalized multiple factors that induced C2C12 myotube atrophy and cachexia-induced skeletal muscle wasting. Notably and to the best of our knowledge, this is the first time that matrine has been demonstrated to downregulate expression of MuRF1 and MAFbx in C2C12 myotubes and skeletal muscle, and that activation of the PI3K/Akt signaling pathway is a potential mechanism of matrine activity in skeletal muscle.

Cancer cachexia has typical characteristics, including loss of body weight, muscle and adipose wasting, weakness, and anorexia (1,2). In previous studies, inflammatory infiltration has been suggested as the main cause of muscle wasting (39-41). However, there is evidence that inflammation does not associate well with cancer cachexia-induced muscle wasting and prolongation of life expectancy, and the Evans publication (30,42) to further establish a comprehensive definition did not include cytokines. Inflammatory factors are derived from tumor cells and activated immune cells (43). In the present study, serum inflammatory cytokines were downregulated by matrine, which was probably one of its benefits. However, the most important finding was that matrine decreased the expression of E3 ubiquitin ligases in skeletal muscle, which is direct evidence of its anti-muscle atrophy effect and is consistent with the increase in skeletal muscle mass and myofiber CSA. Furthermore, matrine ameliorated other cancer cachexia symptoms by increasing body, fat and organ weights. In summary, the results demonstrated that matrine is a potential drug for preventing cancer cachexia symptoms, particularly for skeletal muscle atrophy in mice.

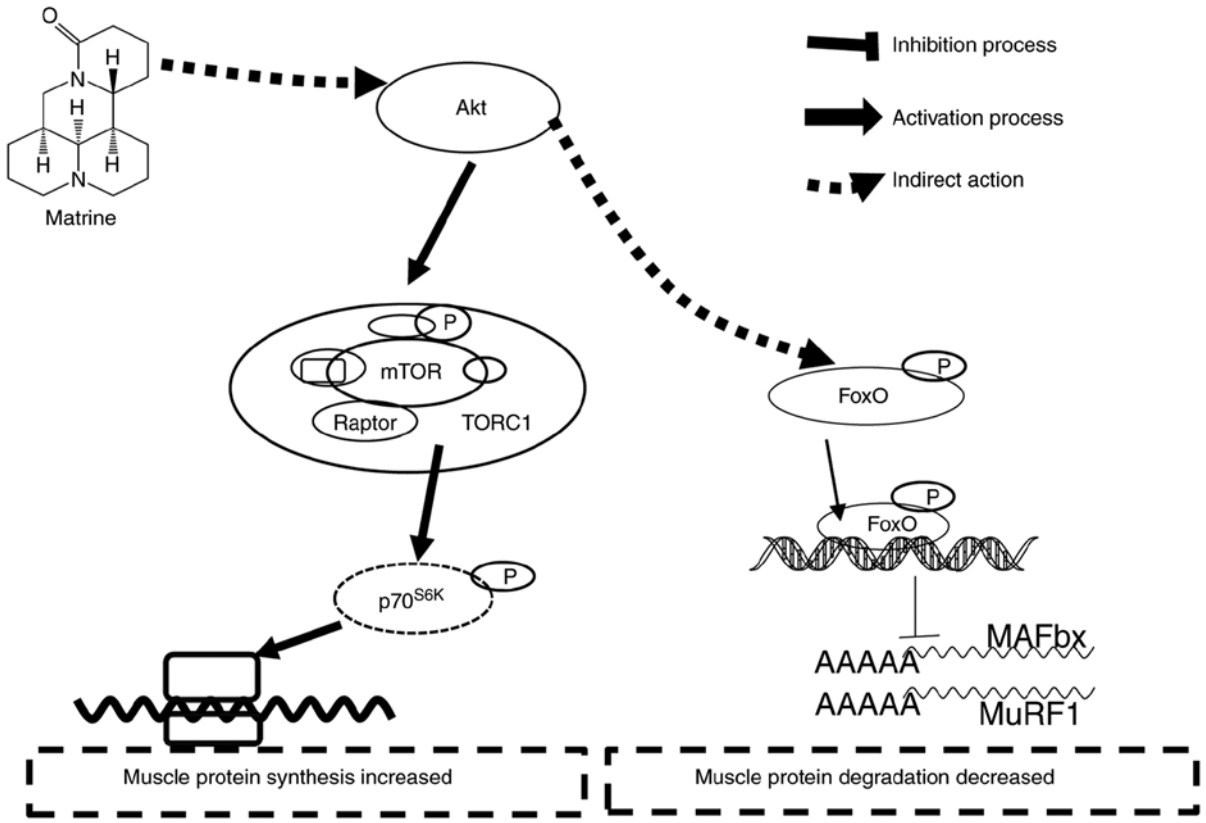

Figure 9. Possible mechanism of matrine on inhibiting skeletal muscle atrophy. Through increasing phosphorylation of key proteins, matrine activates the Akt/mTOR/FoxO3α signaling pathway; therefore, increased muscle protein synthesis and decreased protein degradation occurs.

Matrine has been reported to exhibit acute toxicity in Kunming mice at 80 mg/kg/day (44), and developmental toxicity and neurotoxicity in zebrafish embryos (45). However, matrine was verified to exhibit beneficial effects on hepatitis, cardiac injury and fibrotic diseases (21-23). Therefore, appropriate concentrations for the treatment of C2C12 myoblasts and myotubes need to be investigated. The current CCK-8 assay results demonstrated that matrine exhibited no significant toxicity on C2C12 myocytes below 0.203 mM. Myocytes and myotubes are two different types of C2C12 cells and they have different sensitivities to stimulation (46). Levels of MHC, the main structural protein of myotubes, are mediated by MuRF1, which interacts with MHC and controls its half-life (47). The present RT-qPCR results revealed that <0.2 mM matrine exhibited no negative influence on MHC subfamily mRNA expression levels in myotubes. However, 0.1 mM matrine upregulated mRNA expression of MHC Ib, while it downregulated MHC Ib andIIx at 0.4 mM. C2C12 multinucleate myotubes are formed by myocyte fusion along the axis direction. Myogenic genes, including MyoD, MyoG, Myf5 and Mrf4, serve an important role in this process (20). Dex degrades MyoD by upregulation of atrogin-1, and this decreases protein synthesis and increases skeletal muscle wasting (48). The expression levels of myogenic genes reflect the differentiation potency of myocytes. In the current study, matrine promoted MyoD expression with or without Dex treatment, and this effect mostly reflected its influence on myotube diameter and fusion index. One difference is that a higher concentration of matrine (0.8 mM) produced the highest fusion index, while decreasing the expression of MyoD. This suggests that giant and irregular myotube formation may not reflect healthy myocyte differentiation. These results revealed that matrine may benefit C2C12 cells *in vitro* at <0.4 mM.

Typically, after culture in 2% horse serum for 3-5 days, C2C12 myocytes fuse to form myotubes. Subsequently, although the differentiation medium is replaced daily, the myotubes gradually atrophy a few days later (data not shown). MHC is distributed widely in myotubes (49). Therefore, MHC immunostaining reveals the outline of the myotubes and decreased MHC is a marker of muscle atrophy. Dex, TNFα and CM are often used to establish muscle or myotube atrophy models (31-33). In the present study, decreases in apoptosis and diameter of myotubes caused by these stimulants were completely reversed by matrine. This suggests that matrine serves an important role in modulating a common pathway of the different factors that cause myotube atrophy. Dex-induced skeletal muscle atrophy is caused by upregulation of atrogin-1 and MuRF1 via specific regulators, including FoxO and NF-κB (50), and Dex upregulates the activity and mRNA expression of myostatin (30). Consistent with these previous findings, both western blots and double immunostaining suggested that Dex upregulated MuRF1 protein, MAFbx protein and myostatin mRNA in C2C12 myotubes (Fig. S1). Co-treatment with matrine and Dex demonstrated that MuRF1 and MAFbx protein, and myostatin mRNA were downregulated to much lower levels, which suggests that the progression of myotube atrophy was inhibited.

Several signaling pathways are associated with skeletal muscle hypertrophy and atrophy, involving the control of protein synthesis and degradation (51). In general, the Akt/mTOR and MAPK pathways are inhibited during muscle atrophy, while FoxO and NF-κB are activated (17,52). Upon dephosphorylation, FoxO translocates to the nucleus as a transcription factor, thereby upregulating E3 ubiquitin ligase (52). When FoxO activation is inhibited by RNAi in mouse muscles *in vivo*, both atrogin-1 induction during starvation and myotube atrophy induced by glucocorticoids are prevented (19). Akt is a downstream target of PI3K, which in turn leads to activation of mTOR, followed by activation of p70S6K and PHAS-1/4E-BP1; this promotes protein synthesis through increases in translation initiation and elongation (15). Consistent with this, in the present study of C2C12 myotubes, Dex significantly decreased the relative levels of p-Akt, p-mTOR and p-FoxO3α. However, matrine-treatment largely reversed the phosphorylation of these signal proteins, which could be attenuated by wortmannin, a PI3K inhibitor frequently used for blocking the PI3K/Akt pathway. Combined with the upregulation of the two E3 ligases with wortmannin-treatment, matrine possibly exerts an important effect on the Akt/mTOR/FoxO3α signaling pathway. There is another report that matrine inhibits the phosphorylation of FoxO3α, which induces apoptosis of prostate cancer cells (27). Therefore, the effects of matrine on C2C12 myotubes and cancer cells may be different, which helps explain why matrine alleviated the CT26 tumor burden in the current study. However, more in-depth studies are required. Collectively, the anti-muscle atrophy effects of matrine appear to involve the Akt/mTOR/FoxO3α signaling pathway (Fig. 9).

However, there are certain limitations of the current study. First, the effect of matrine was only identified on CT26 tumor cachexia. Future research should focus on the effect of matrine on more cancer cachexia models. Second, the effect of matrine on patients with cancer cachexia would be more convincing. However, a small number of patients with matrine-treated cancer cachexia receive surgery; therefore, few clinical samples would be accessible. Along with the increasing popularity of treating cancer cachexia with matrine, we hope to obtain more clinical samples and perform more in-depth research in the future.

In conclusion, the present study predominantly investigated the anti-muscle atrophy effects and mechanism of matrine in C2C12 myotubes, and the effects of matrine were verified in CT26-induced cachexia mice. Matrine substantially improved CT26 colon adenocarcinoma-induced skeletal muscle atrophy by preserving the mass and CSA of myofibers. Matrine-treatment also significantly increased C2C12 myoblast differentiation and attenuated myotube atrophy. Notably, to the best of our knowledge, matrine was demonstrated for the first time to downregulate expression of MuRF1 and MAFbx in cancer cachexia skeletal muscle, and matrine's effect on the Akt/mTOR/FoxO3α signaling pathway was identified to be involved in this phenomenon.

Acknowledgements

The authors wish to thank Ms Jingxian Zhang and Ms Dan Feng (Department of Pharmacy, Shanghai Jiao Tong University Affiliated Sixth People's Hospital, Shanghai, China), who provided kind assistance with the animal experiments.

Funding

This work was supported by grants from the National Science Foundation of China (grant nos. 81873042 and 81872494).

Availability of data and materials

The datasets used during the present study are available from the corresponding author upon reasonable request.

Authors' contributions

LiC, YH, QY JH and CG participated in the research design. LiC, LinC and BX performed the experiments. JLi, JLu and BX contributed the reagents, materials and analysis tools. LiC, JLi, QY, JLu, LW and CG acquired and analysed the data. JLu and JH interpreted the data. LiC, LW, JLu and JH wrote and proofread the manuscript. All authors read and approved the manuscript and agree to be accountable for all aspects of the research in ensuring that the accuracy or integrity of any part of the work are appropriately investigated and resolved.

Ethics approval and consent to participate

All procedures involving animals and their care in the current study were approved by the Animal Care Committee of Shanghai Jiao Tong University Affiliated Sixth People's Hospital (Shanghai, China) in accordance with institutional requirements and Chinese government guidelines for animal experiments.

Patient consent for publication

Not applicable.

Competing interests

The authors declare that they have no competing interests.

References

1. Baracos VE, Martin L, Korc M, Guttridge DC and Fearon KCH: Cancer-associated cachexia. Nat Rev Dis Primers 4: 17105, 2018.
2. Fearon K, Strasser F, Anker SD, Bosaeus I, Bruera E, Fainsinger RL, Jatoi A, Loprinzi C, MacDonald N, Mantovani G, *et al*: Definition and classification of cancer cachexia: An international consensus. Lancet Oncol 12: 489-495, 2011.
3. Argiles JM, Busquets S, Stemmler B and Lopez-Soriano FJ: Cancer cachexia: Understanding the molecular basis. Nat Rev Cancer 14: 754-762, 2014.
4. Daly LE, Ní Bhuachalla ÉB, Power DG, Cushen SJ, James K and Ryan AM: Loss of skeletal muscle during systemic chemotherapy is prognostic of poor survival in patients with foregut cancer. J Cachexia Sarcopenia Muscle 9: 315-325, 2018.
5. Fearon K, Arends J and Baracos V: Understanding the mechanisms and treatment options in cancer cachexia. Nat Rev Clin Oncol 10: 90-99, 2013.
6. Yang QJ, Zhao JR, Hao J, Li B, Huo Y, Han YL, Wan LL, Li J, Huang J, Lu J, *et al*: Serum and urine metabolomics study reveals a distinct diagnostic model for cancer cachexia. J Cachexia Sarcopenia Muscle 9: 71-85, 2018.

7. Quanjun Y, Genjin Y, Lili W, Bin L, Jin L, Qi Y, Yan L, Yonglong H, Cheng G and Junping Z: Serum metabolic profiles reveal the effect of formoterol on cachexia in tumor-bearing mice. Mol Biosyst 9: 3015-3025, 2013.
8. Chen T, Li B, Xu Y, Meng S, Wang Y and Jiang Y: Luteolin reduces cancerinduced skeletal and cardiac muscle atrophy in a Lewis lung cancer mouse model. Oncol Rep 40: 1129-1137, 2018.
9. Chen X, Wu Y, Yang T, Wei M, Wang Y, Deng X, Shen C, Li W, Zhang H, Xu W, *et al*: Salidroside alleviates cachexia symptoms in mouse models of cancer cachexia via activating mTOR signalling. J Cachexia Sarcopenia Muscle 7: 225-232, 2016.
10. Argiles JM: The 2015 ESPEN Sir david cuthbertson lecture: Inflammation as the driving force of muscle wasting in cancer. Clin Nutr 36: 798-803, 2017.
11. Lecker SH, Jagoe RT, Gilbert A, Gomes M, Baracos V, Bailey J, Price SR, Mitch WE and Goldberg AL: Multiple types of skeletal muscle atrophy involve a common program of changes in gene expression. FASEB J 18: 39-51, 2004.
12. Crossland H, Constantin-Teodosiu D, Gardiner SM, Constantin D and Greenhaff PL: A potential role for Akt/FOXO signalling in both protein loss and the impairment of muscle carbohydrate oxidation during sepsis in rodent skeletal muscle. J Physiol 586: 5589-5600, 2008.
13. Bodine SC, Latres E, Baumhueter S, Lai VK, Nunez L, Clarke BA, Poueymirou WT, Panaro FJ, Na E, Dharmarajan K, *et al*: Identification of ubiquitin ligases required for skeletal muscle atrophy. Science 294: 1704-1708, 2001.
14. Glass DJ: Signaling pathways perturbing muscle mass. Curr Opin Clin Nutr Metab Care 13: 225-229, 2010.
15. Bodine SC, Stitt TN, Gonzalez M, Kline WO, Stover GL, Bauerlein R, Zlotchenko E, Scrimgeour A, Lawrence JC, Glass DJ and Yancopoulos GD: Akt/mTOR pathway is a crucial regulator of skeletal muscle hypertrophy and can prevent muscle atrophy in vivo. Nat Cell Biol 3: 1014-1019, 2001.
16. Cai D, Frantz JD, Tawa NJ, Melendez PA, Oh BC, Lidov HG, Hasselgren PO, Frontera WR, Lee J, Glass DJ and Shoelson SE: IKKbeta/NF-kappaB activation causes severe muscle wasting in mice. Cell 119: 285-298, 2004.
17. McFarlane C, Plummer E, Thomas M, Hennebry A, Ashby M, Ling N, Smith H, Sharma M and Kambadur R: Myostatin induces cachexia by activating the ubiquitin proteolytic system through an NF-kappaB-independent, FoxO1-dependent mechanism. J Cell Physiol 209: 501-514, 2006.
18. Zimmers TA, Fishel ML and Bonetto A: STAT3 in the systemic inflammation of cancer cachexia. Semin Cell Dev Biol 54: 28-41, 2016.
19. Sandri M, Sandri C, Gilbert A, Skurk C, Calabria E, Picard A, Walsh K, Schiaffino S, Lecker SH and Goldberg AL: Foxo transcription factors induce the atrophy-related ubiquitin ligase atrogin-1 and cause skeletal muscle atrophy. Cell 117: 399-412, 2004.
20. Kitzmann M, Carnac G, Vandromme M, Primig M, Lamb NJ and Fernandez A: The muscle regulatory factors MyoD and myf-5 undergo distinct cell cycle-specific expression in muscle cells. J Cell Biol 142: 1447-1459, 1998.
21. Long Y, Lin XT, Zeng KL and Zhang L: Efficacy of intramuscular matrine in the treatment of chronic hepatitis B. Hepatobiliary Pancreat Dis Int 3: 69-72, 2004.
22. Li X, Wang X, Guo Y, Deng N, Zheng P, Xu Q, Wu Y and Dai G: Regulation of endothelial nitric oxide synthase and asymmetric dimethylarginine by matrine attenuates isoproterenol-induced acute myocardial injury in rats. J Pharm Pharmacol 64: 1107-1118, 2012.
23. Li Y, Wang B, Zhou C and Bi Y: Matrine induces apoptosis in angiotensin II-stimulated hyperplasia of cardiac fibroblasts: Effects on Bcl-2/Bax expression and caspase-3 activation. Basic Clin Pharmacol Toxicol 101: 1-8, 2007.
24. Shao H, Yang B, HU R and Wang Y: Matrine effectively inhibits the proliferation of breast cancer cells through a mechanism related to the NF-κB signaling pathway. Oncol Lett 6: 517-520, 2013.
25. Zhang S, Cheng B, Li H, Xu W, Zhai B, Pan S, Wang L, Liu M and Sun X: Matrine inhibits proliferation and induces apoptosis of human colon cancer LoVo cells by inactivating Akt pathway. Mol Biol Rep 41: 2101-2108, 2014.
26. Li Q, Lai Y, Wang C, Xu G, He Z, Shang X, Sun Y, Zhang F, Liu L and Huang H: Matrine inhibits the proliferation, invasion and migration of castration-resistant prostate cancer cells through regulation of the NF-κB signaling pathway. Oncol Rep 35: 375-381, 2016.
27. Bai S, Chen T, Yu X, Luo M, Chen X, Lin C, Lai Y and Huang H: The specific killing effect of matrine on castration-resistant prostate cancer cells by targeting the Akt/FoxO3a signaling pathway. Oncol Rep 37: 2819-2828, 2017.
28. Zhang Y, Wang S, Li Y, Xiao Z, Hu Z and Zhang J: Sophocarpine and matrine inhibit the production of TNF-alpha and IL-6 in murine macrophages and prevent cachexia-related symptoms induced by colon26 adenocarcinoma in mice. Int Immunopharmacol 8: 1767-1772, 2008.
29. Donohoe CL, Ryan AM and Reynolds JV: Cancer cachexia: Mechanisms and clinical implications. Gastroenterol Res Pract 2011: 601434, 2011.
30. Muscaritoli M, Anker SD, Argiles J, Aversa Z, Bauer JM, Biolo G, Boirie Y, Bosaeus I, Cederholm T, Costelli P, *et al*: Consensus definition of sarcopenia, cachexia and pre-cachexia: Joint document elaborated by Special Interest Groups (SIG) 'cachexia-anorexia in chronic wasting diseases' and 'nutrition in geriatrics'. Clin Nutr 29: 154-159, 2010.
31. Kim H, Jang M, Park R, Jo D, Choi I, Choe J, Oh WK and Park J: Conessine treatment reduces dexamethasone-induced muscle atrophy by regulating MuRF1 and atrogin-1 expression. J Microbiol Biotechnol 28: 520-526, 2018.
32. Jackman RW, Floro J, Yoshimine R, Zitin B, Eiampikul M, El-Jack K, Seto DN and Kandarian SC: Continuous release of tumor-derived factors improves the modeling of cachexia in muscle cell culture. Front Physiol 8: 738, 2017.
33. Xi QL, Zhang B, Jiang Y, Zhang HS, Meng QY, Chen Y, Han YS, Zhuang QL, Han J, Wang HY, *et al*: Mitofusin-2 prevents skeletal muscle wasting in cancer cachexia. Oncol Lett 12: 4013-4020, 2016.
34. Aulino P, Berardi E, Cardillo VM, Rizzuto E, Perniconi B, Ramina C, Padula F, Spugnini EP, Baldi A, Faiola F, *et al*: Molecular, cellular and physiological characterization of the cancer cachexia-inducing C26 colon carcinoma in mouse. BMC Cancer 10: 363, 2010.
35. Yang Q, Wan L, Zhou Z, Li Y, Yu Q, Liu L, Li B and Guo C: Parthenolide from parthenium integrifolium reduces tumor burden and alleviate cachexia symptoms in the murine CT-26 model of colorectal carcinoma. Phytomedicine 20: 992-998, 2013.
36. Livak KJ and Schmittgen TD: Analysis of relative gene expression data using real-time quantitative PCR and the 2(-Delta Delta C(T)) method. Methods 25: 402-408, 2001.
37. Neefjes ECW, van den Hurk RM, Blauwhoff-Buskermolen S, van der Vorst MJDL, Becker-Commissaris A, de van der Schueren MAE, Buffart LM and Verheul HMW: Muscle mass as a target to reduce fatigue in patients with advanced cancer. J Cachexia Sarcopenia Muscle 8: 623-629, 2017.
38. Carr RM, Enriquez-Hesles E, Olson RL, Jatoi A, Doles J and Fernandez-Zapico ME: Epigenetics of cancer-associated muscle catabolism. Epigenomics: Sep 25, 2017 (Epub ahead of print). doi: 10.2217/epi-2017-0058 2017.
39. Haddad F, Zaldivar F, Cooper DM and Adams GR: IL-6-induced skeletal muscle atrophy. J Appl Physiol (1985) 98: 911-917, 2005.
40. Deans C and Wigmore SJ: Systemic inflammation, cachexia and prognosis in patients with cancer. Curr Opin Clin Nutr Metab Care 8: 265-269, 2005.
41. Patel HJ and Patel BM: TNF-α and cancer cachexia: Molecular insights and clinical implications. Life Sci 170: 56-63, 2017.
42. Scheede-Bergdahl C, Watt HL, Trutschnigg B, Kilgour RD, Haggarty A, Lucar E and Vigano A: Is IL-6 the best pro-inflammatory biomarker of clinical outcomes of cancer cachexia? Clin Nutr 31: 85-88, 2012.
43. Fearon KC, Glass DJ and Guttridge DC: Cancer cachexia: Mediators, signaling, and metabolic pathways. Cell Metab 16: 153-166, 2012.
44. Wang XY, Liang L, Chang JL, Yang MH and Li ZG: Toxicity of matrine in Kunming mice. Nan Fang Yi Ke Da Xue Xue Bao 30: 2154-2155, 2010 (In Chinese).
45. Lu ZG, Li MH, Wang JS, Wei DD, Liu QW and Kong LY: Developmental toxicity and neurotoxicity of two matrine-type alkaloids, matrine and sophocarpine, in zebrafish (Danio rerio) embryos/larvae. Reprod Toxicol 47: 33-41, 2014.
46. Burattini S, Ferri P, Battistelli M, Curci R, Luchetti F and Falcieri E: C2C12 murine myoblasts as a model of skeletal muscle development: Morpho-functional characterization. Eur J Histochemistry 48: 223-233, 2004.
47. Clarke BA, Drujan D, Willis MS, Murphy LO, Corpina RA, Burova E, Rakhilin SV, Stitt TN, Patterson C, Latres E and Glass DJ: The E3 Ligase MuRF1 degrades myosin heavy chain protein in dexamethasone-treated skeletal muscle. Cell Metab 6: 376-385, 2007.

48. Castillero E, Alamdari N, Lecker SH and Hasselgren PO: Suppression of atrogin-1 and MuRF1 prevents dexamethasone-induced atrophy of cultured myotubes. Metabolism 62: 1495-1502, 2013.
49. Adams GR, Hather BM, Baldwin KM and Dudley GA: Skeletal muscle myosin heavy chain composition and resistance training. J Appl Physiol (1985) 74: 911-915, 1993.
50. Desler MM, Jones SJ, Smith CW and Woods TL: Effects of dexamethasone and anabolic agents on proliferation and protein synthesis and degradation in C2C12 myogenic cells. J Anim Sci 74: 1265-1273, 1996.
51. Schiaffino S, Dyar KA, Ciciliot S, Blaauw B and Sandri M: Mechanisms regulating skeletal muscle growth and atrophy. FEBS J 280: 4294-4314, 2013.
52. Lokireddy S, McFarlane C, Ge X, Zhang H, Sze SK, Sharma M and Kambadur R: Myostatin induces degradation of sarcomeric proteins through a Smad3 signaling mechanism during skeletal muscle wasting. Mol Endocrinol 25: 1936-1949, 2011.